Role of TNF-α and the NF-κB pathway in drug-induced organ injuries

Benedetti, G.O.E.

Citation

Cover Page

Universiteit Leiden

Author: Benedetti, Giulia
Title: Role of TNF-α and the NF-κB pathway in drug-induced organ injuries
Issue Date: 2013-05-07

7

A live-cell imaging-based NF-κB nuclear translocation RNAi screen identifies novel regulators of TNF-α-induced apoptosis through control of the (de)ubiquitinase A20

Giulia Benedetti*, Lisa Fredriksson*, Bram Herpers*, Marjo de Graauw and Bob van de Water

* Equal contribution

Division of Toxicology, Leiden/Amsterdam Center for Drug Research, Leiden University, The Netherlands

Manuscript in preparation

Abstract

Stimulation of cells with the cytokine tumor necrosis factor alpha (TNF-α) triggers cytoplasmic-to-nuclear oscillation of the dimeric transcription factor NF-kappaB (NF-κB). In the nucleus, NF-κB stimulates transcription of its own response inhibitors, IkappaBalpha (IκBα) and the (de)ubiquitinase A20. The concerted induction of IκBα and A20 functions to prevent over-activation of the response and the time-dependent inactivation is observed as a dampened NF-κB nuclear oscillation pattern. The number of nuclear oscillations dictates the transcription of downstream pro-inflammatory, anti-oxidant and anti-apoptotic genes. The number of nuclear translocation events is markedly reduced under hepatotoxic drug (diclofenac) exposure conditions in association with enhanced apoptosis. To understand the mechanism of the perturbed oscillatory response, we used a live-cell imaging-based siRNA screen to identify individual kinases, (de)ubiquitinases and sumoylases that control the NF-κB oscillatory response. We applied high content confocal laser scan microscopy in combination with multi-parametric image analysis to follow the NF-κB oscillation in ~300 individual cells per condition simultaneously. Out of the ~1500 genes screened, we identified 115 that significantly affected the NF-κB oscillatory response. Using 4 individual siRNAs, we confirmed the action for 46 genes, which affected: (i) the amplitude or duration of nuclear oscillations; (ii) the time between oscillations, leading to an increase or decrease of the number of nuclear translocations; or (iii) an inhibition of the response altogether. In this last category we identified five genes, three novel, whose reduced expression protected against the diclofenac/TNF-α-induced apoptosis. Interestingly, the knockdown of four of these genes led to a basic up-regulation of A20 expression. In accordance, A20 knockdown promoted the NF-κB oscillation and enhanced apoptosis. Double knockdown experiments indicated a direct relationship between these four genes and A20 in the control of the NF-κB activation. These findings indicate that the (de)ubiquitinase A20 is a master regulator in the life-death decision upon TNF-α stimulation in drug-induced hepatotoxic responses, which, in turn, is kept under control by a network of genes that control its expression level.

1. Introduction

The dimeric transcription factor nuclear factor-κB (NF-κB) controls the expression of a wide array of genes that play an important role in many stages of both physiology and disease. The activity of NF-κB is crucial in the host-pathogen response by transcribing anti-oxidant and pro-inflammatory genes and thereby activating the

innate and adaptive immune response (1). In addition, the activity of NF-κB has been associated with disease states such as cancer, chronic inflammatory diseases and atherosclerosis (2). The malignant role of NF-κB arises from improper regulation of its activation. Enhanced activation of NF-κB leads to over-expression of genes responsible for proliferation, angiogenesis, metastasis, tumor promotion, inflammation and suppression of apoptosis, which gives the transcription factor its tumorigenic properties (3, 4). Yet on the other hand, inhibition of NF-κB activity has been associated with toxicity of drugs (5, 6).

NF-κB is activated by canonical and atypical signalling pathways. The canonical pathway is typically activated by pro-inflammatory stimuli such as the cytokines tumor necrosis factor-α (TNF-α) and interleukin-1β (IL-1β) that bind to their respective receptors TNFR and IL-1R. Receptor activation is followed by the assembly of a signalling complex composed of several adaptor molecules, ubiquitin ligases and kinases to promote activation of the IKK-complex, the rate-limiting step of NF-κB pathway signalling. The IKK-complex consists of the catalytic subunits CHUK (IKKα) and IKBKB (IKKβ) and the regulatory subunit IKBKG (IKKγ or NEMO) (7). The active IKK complex phosphorylates the inhibitor of NF-κB, IκB, which is subsequently poly-ubiquitinated and degraded by the proteasome. This process unmasks the nuclear localization signal in NF-κB, allowing nuclear translocation and initiation of NF-κB driven gene transcription (8). De-regulation of the IKK-complex is observed in different cancers, for example through activating mutations in NF-κB signalling promoting genes such as the NF-κB inducing kinase (NIK; MAP3K14) or inactivating mutations in NF-κB signalling repressors such as the deubiquitinase cylindromatosis (CYLD) (9), indicating that NF-κB activity requires tight regulation to control normal cellular physiology.

To understand this regulatory control, the NF-κB pathway has been subject to different screening approaches to further decipher its intracellular signalling. Gain- and loss-of-function screens based on NF-κB luciferase reporter constructs (10, 11) were performed using cDNAs (10) or RNA-interference (siRNAs) (11, 12). These end-point assay screens focused on the prolonged NF-κB activity, and were unable to unravel the complex regulatory mechanisms involved in NF-κB activity that determine the spatial and temporal behavior of NF-κB after receptor stimulation.

The nuclear translocation of NF-κB is an oscillatory response that is controlled by feedback control mechanisms and varies between individual cells. Importantly, these NF-κB oscillations determine the extent and levels of gene transcription (13-15). These oscillatory responses vary within a cell population and is dependent on regulation by post-translational modifications such as phosphorylation, (de)ubiquitination

and sumoylation (16). TNF-α-induced activation requires K63 and linear (poly-)ubiquitination chains to allow (auto-)phosphorylation of the IKK kinases to promote K48 linked poly-ubiquitination of IκB (8). Termination depends on deubiquitination as well as ubiquitination processes, as exemplified by the protein A20 (TNFAIP3). A20 deubiquitinates the activating K63 chains from receptor-interacting protein 1 (RIP1), a TNFR associated kinase upstream of the IKK-complex, and replaces these by K48 chains, marking RIP1 for proteasomal degradation (17, 18). As TNFAIP3 and NFKBIA (IκBα) are two of the principle early target genes of NF-κB, this provides a very important negative feedback loop to control NF-κB activation and constitutes the reason for the dampened oscillatory translocation pattern of NF-κB (19). Also drugs that cause liver failure in patients strongly affect the NF-κB oscillatory response (5).

In the current manuscript we searched for novel regulatory components of the oscillatory nuclear translocation response of the canonical NF-κB subunit p65 (RelA) upon exposure to the pro-inflammatory cytokine TNF-α. We studied this in the context of drug-induced liver injury responses. Here we present an advanced screening approach to quantitatively determine the effect of individual gene knockdowns on the temporal and spatial behavior of NF-κB in single cells as well as at the population level using combined RNAi and using live high content confocal imaging of green fluorescent protein tagged p65 (GFP-p65), in a HepG2 cell background. We identified several novel genes that are essential for the regulation of A20 protein levels, which thereby not only control NF-κB oscillation, but also the susceptibility of TNF-α-mediated enhancement of drug-induced toxicity.

2. Material and methods
2.1. Reagents and antibodies

Human recombinant TNF-α was acquired from R&D Systems (Abingdon, UK). Diclofenac sodium and the antibody against tubulin were from Sigma-Aldrich (Zwijndrecht, The Netherlands). AnnexinV-Alexa633 and AnnexinV-Alexa561 were made as described (20). The antibody against phospho-specific IκBα was from Cell Signalling (Bioké, Leiden, The Netherlands). The antibody against A20 was from Santa Cruz (Tebu-Bio, Heerhugowaard, The Netherlands). The bromo phenol blue solution was from Merck (Merck Millipore, Amsterdam Zuidoost, The Netherlands).

2.2. Cell culture

Human hepatoma HepG2 cells were obtained from American Type Culture Collection (clone HB-8065, ATCC, Wesel, Germany). HepG2 cells stably expressing GFP-p65 (NF-κB subunit) were created by 400 µg/ml G418 selection upon pEGFP-C1-p65 transfection using Lipofectamine™ 2000 (Invitrogen, Breda, Netherlands). HepG2 BAC IκBα-GFP cells were generated by bacterial artificial chromosome (BAC) recombineering (21,22). Upon validation of correct C-terminal integration of the GFP-cassette by PCR, the BAC-GFP construct was transfected using Lipofectamine™ 2000. Stable HepG2 BAC IκBα-GFP cells were obtained by 500 µg/ml G418 selection. For all experiments the cells were cultured in Dulbecco's modified Eagle's medium (DMEM) supplemented with 10% (v/v) fetal bovine serum (FBS), 25 U/ml penicillin, and 25 µg/ml streptomycin between passages 5 and 20.

2.3. RNA interference

Transient knockdowns of individual target genes were achieved using siGENOME SMARTpool siRNA reagents in the primary screen or single siRNA sequences in the secondary deconvolution screen (50 nM; Dharmacon Thermo Fisher Scientific, Landsmeer, Netherlands). HepG2 cells were transfected using INTERFERin siRNA transfection reagent according to the manufacturer's procedures (Polyplus transfection, Leusden, Netherlands) and left for 72 hours to achieve maximal knockdown before treatment. The negative controls were siGENOME non-targeting pool #1, caspase-8 and mock (INTERFERin only) transfection.

2.4. Exposures

Prior to imaging, nuclei were stained with 100 ng/ml Hoechst 33342 in complete DMEM for 45 minutes. The cells were then exposed to Diclofenac 500 µM or DMSO 0.2% for 8 hours. The cells were then challenged with human TNF-α (10 ng/ml).

2.5. Live Cell Imaging of GFPp65 and GFP-IκBα in HepG2 Cells

The GFP-p65 nuclear translocation response and IκBα-GFP level response upon 10 ng/ml human TNF-α challenge was followed for a period of 6 hours by automated confocal imaging every 6 minutes (Nikon TiE2000, Nikon, Amstelveen, Netherlands).

Quantification of the nuclear/cytoplasmic ratio of GFPp65 intensity in individual cells was performed using an algorithm for ImageJ (Z. Di, B. Herpers, L. Fredriksson, K. Yan, B. van de Water, F.J. Verbeek and J.H.N. Meerman, submitted).

2.6. Translocation response class definition and hit definition

For the primary screen, the amplitudes of the individual translocation response tracks were normalized to their intrinsic response maxima (=1) and minima (=0) to be able to compare the timing of the nuclear translocation events versus the plate average. For the secondary screen, non-normalized data were used. Four different classes were defined according to the type of nuclear p65 oscillation response: increased, no oscillation, decreased and different compared to the oscillation observed with control siRNA. Each class used a different set of five specific parameters (Fig. 1A). For each targeted gene, a Pearson's chi-squared cumulative statistic was calculated from the set of five parameters of each class and p-values were obtained by comparing the value of the statistic to a chi-squared distribution. Targeted genes obtaining a p-value lower than or equal to 0.001 were considered as hits.

2.7. Apoptosis measurements

Apoptosis was determined by the live cell apoptosis assay previously described (20) (5). The relative Annexin V fluorescence intensity per image was quantified using Image Pro (Media Cybernetics, Bethesda, MD) and normalized to the number of nuclei or cell area to obtain the estimated percentage of apoptosis.

2.8. Western Blot

Cells were harvested in sample buffer (6 times diluted bromo phenol blue solution with β-mercaptoethanol). The samples were subjected to protein separation, blotted on Immobilon-P (Millipore, Amsterdam, The Netherlands). Phosphorylated IκBα was detected using the Tropix Western-Star kit™ (Applied Biosystems) following manufacturer's protocol. For tubulin and A20, the membranes were blocked for 1h at room temperature in milk powder 5% (w/v) in Tris-buffered saline/Tween 20 (TBS-T). Primary antibody incubation was done overnight at 4°C followed by incubation with cy5-labeled secondary or horseradish peroxidase-conjugated antibodies (Jackson Immunoresearch, Newmarket, UK) in 1% BSA in TBS-T for 1 h at room temperature.

Protein signals were detected with ECL (GE Healthcare) followed by film detection for A20 or by visualization on the Typhoon 9400 imager (GE Healthcare, Diegem, Belgium) for tubulin.

2.9. Statistical procedures

All numerical results are expressed as mean ± standard error of the mean (S.E.M.). Statistical significance was determined by GraphPad Prism using an unpaired t-test, * P≤0.05, ** P≤0.01, *** P≤0.001. Heatmap representations and hierarchical clustering (using Pearson correlation) were performed using the MultiArray Viewer software.

3.   Results
3.1. NF-κB nuclear oscillation phenotype siRNA screening in HepG2 cells

Stimulation of cells with TNF-α initiates nuclear translocation oscillation of the NF-κB transcription factor. To better understand this process in human liver cells and identify genes controlling the oscillation pattern, we created a stable HepG2 reporter line using GFP-tagged NF-κB subunit p65/RelA. Time-lapse confocal microscopy showed that the nuclear translocation of GFP-p65 is transient and follows a dampened oscillation at set time intervals, largely due to NF-κB-dependent transcription of IκBα (19). Under control conditions, the initial translocation peaks at 30 minutes after TNF-α (10 ng/ml) stimulation, followed by a second and third peak at 120 minute intervals (Fig. 1A, top). This oscillation pattern was maximal at 10 ng/ml TNF-α (data not shown). RNAi-mediated knock-down of two key NF-κB regulatory genes A20 and IκBα resulted in changes in the oscillation pattern of NF-κB. While A20 knockdown (Supplemental Data S1) slightly decreased the time-interval between oscillations, leading to increased oscillation, knockdown of IκBα (Supplemental Data S1) almost completely inhibited NF-κB oscillation in association with enhanced levels of p65-GFP expression (Fig. 1A, middle). An 8 hour pre-incubation of HepG2 cells with 500 μM diclofenac, a compound known to inhibit TNF-α-mediated NF-κB nuclear translocation (5), increased the time interval between peaks, implicating decreased NF-κB oscillation (Fig. 1A, bottom; (5)). To distinguish these four different NF-κB oscillation phenotypes (control, increased oscillation, decreased oscillation and no oscillation) from one another, we established a pipeline of automated image segmentation and GFP-p65 nuclear/cytoplasmic ratio quantification for all individual cells within one time-series, followed by extraction
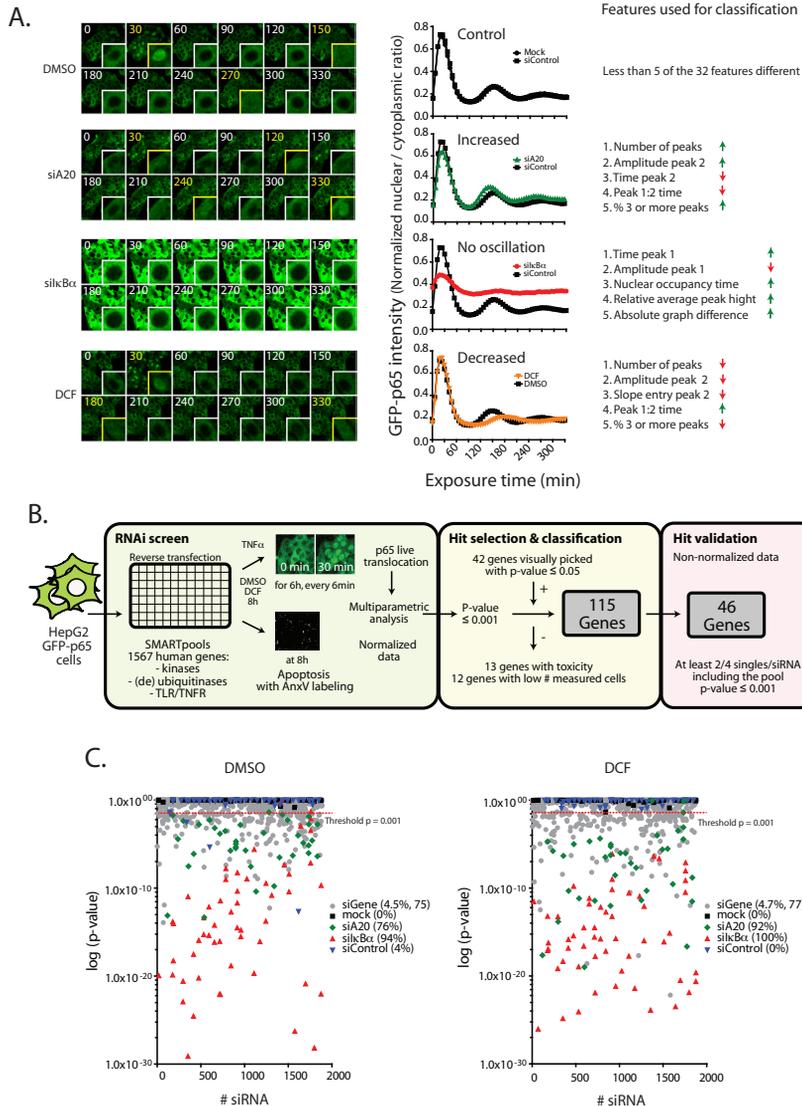
Figure 1. NF-κB oscillation phenotype siRNA screening in HepG2 cells. (A) Representative images of GFP-p65 translocation after TNF-α (10 ng/ml) challenge in HepG2 cells by automated confocal microscopy. Insets: zooms of single cells with an average response in respect to the imaged population. The nuclear translocation events are marked by yellow boxes and the numbers indicate the time in minutes after TNF-α exposure. The nuclear translocation track of each cell was quantified and normalized to its own highest nuclear-to-cytoplasmic ratio (value of 1) and its lowest ratio (0). The average response of the total cell population is presented in the middle panel. The features and their directions that define the response classes (different, increased, decreased and no oscillation) compared to control are shown in the panel to the right. (B) Flowchart of the siRNA screen. (C) P-value distribution of the hits and the positive and negative controls. Under DMSO conditions the true discovery rate was 0.94 and 0.76 for silκBα and siA20 respectively while the false discovery rate was 0.04. Under DCF conditions the corresponding values were, 1, 0.92 and 0 respectively. 4.5% of the screened genes were found to have an effect on the oscillation under DMSO conditions while 4.7% were determined to give a significant effect after DCF pre-exposure.

of 32 distinct oscillation features (Di et al., submitted). We classified the phenotypes based on the direction versus control for at least five oscillation features, (e.g. number of peaks, time between peaks and amplitude of peaks) (Fig. 1A). When more than 5 of the 32 measured oscillation features were distinct from control and the oscillation phenotype did not match any of the other categories, the response was marked as "different oscillation".

Having established an automated system to track, segment and categorize the NF-κB oscillation pattern in individual cells, we set out to identify the genes that are responsible for the timely activity of the NF-κB response by siRNA screening (Fig. 1B). We used siRNAs directed against 779 kinases, 107 de-ubiquitinases and sumoylases, 580 ubiquitin ligases and 123 pre-described players in the TNFR/TLR-driven NF-κB response, under DMSO (control) and diclofenac (DCF) conditions. 22 siRNAs were overlapping in either of the libraries. Annexin-V-Alexa633 labelling of the cells allowed us to exclude the genes that induced apoptosis upon knockdown. For all target genes the oscillation of the GFP-p65 reporter was followed for 6 hours at 6 minute intervals, directly after TNF-α stimulation. Because we were mainly interested in the time between oscillations under control and DCF conditions, we normalized the nuclear/cytoplasmic GFP intensity ratio and separated the analysis for both conditions. Within each condition, we considered genes a potential hit at a p-value below or equal to 0.001, a minimum of in total 35 cells analysed (average number of cells was 184 per condition) and absence of apoptosis. Within this p-value cut-off we could trace back the effect of A20 knockdown under control and DCF conditions in 76% and 92% of the samples, respectively; and the effect of IκBα knockdown in 94% and 100% of the samples (Fig. 1C). Another 42 genes were added from the "different" category, based on visual inspection of the translocation phenotype and taking a p-value of ≤ 0.05 into consideration. In total we re-screened 115 genes using 4 single siRNAs targeting the same gene. In total, 46 genes were confirmed to affect the GFP-p65 oscillation with 2 or more single siRNAs in addition to the pooled siRNAs in either or both DMSO and DCF conditions.

3.2. Functional and phenotypic classification of the siRNA screen hits that control NF-κB oscillation

Out of the 46 confirmed hits, 5 genes, including the known inhibitor of NF-κB activation, UCHL1 (23), decreased the oscillation after knockdown; 7 increased the oscillation, also confirming the inhibitory role for TNFAIP3 (A20) for the activation of

NF-κB; 24 showed no oscillation, including the essential activators of NF-κB IKBKG (IKKγ) and ubiquitin ligase CUL1, needed for the poly-ubiquitination of IκBα (24), and 4 did not fall in the previous three categories, but were significantly different from the controls under DMSO conditions (Fig. 2A-B and Table 1). The oscillation-decreasing effect of DCF was further inhibited by siRNAs targeting the splicing factor PHF5A and the receptor TNFRSF18. Furthermore, 12 siRNAs increased the oscillation, 22 stopped the oscillation, including the siRNA tageting the cyclin-dependent kinase CDK12 that was shown to only decrease the oscillation under DMSO conditions, and 4 had a different oscillation phenotype (Fig. 2B and Table 1). When comparing DF and DMSO conditions, 33 hits were overlapping, 7 were unique for DMSO and 6 for the diclofenac condition at a p-value cut-off of $p<0.001$ (Fig. 2B-C and Table 1). Most hits were kinases and (ubiquitin) ligases, which most often contributed to the "no oscillation" or "decreased" response phenotype (Fig. 2D and 2E).

The strength of our siRNA screening approach is the analysis of the dynamics of the NF-κB response at the single cell level within an entire population of cells. This allows measurement of the population dynamics upon knockdown of our candidate genes (Fig. 3A and 3B). Under control conditions the majority of the cells showed three nuclear translocation events within the imaging period. Yet the siRNA conditions that blocked the oscillation led to profiles with either no, or one shallow oscillation event, as shown with knock-down of our positive control IκBα and knockdown of IKBKG (IKKγ) and TNFRSF1A (TNFR1), two genes necessary for NF-κB activation, (Fig. 3Bi). The decreased oscillation phenotype exhibited mainly 2 or 3 oscillation events, as shown by knockdown of CDK12 and PHF5A, whereas the increased class, best illustrated by knockdown of our positive control TNFAIP3 (A20), showed mostly cells with 3 or 4 oscillations (Fig. 3Bii). Within the profile class of "no oscillation" the number of peaks was vastly reduced and any observable translocation event occurred later than in control cells, at lower amplitude and with a reduced nuclear entry slope. Within the remaining fraction of cells (~30%) that showed more than one nuclear translocation event, the peaks remained shallow, which leads to a reduced dampening between the peaks (Fig. 3Ci). The group of siRNAs that decreased the oscillation also decreased the number of oscillations and increased the time of the first translocation event. Differently from the "no oscillation" class, the profiles within the "decreased" class that included CDK12, RBX1, PHF5A and USP8, all showed an increase in the duration of the initial translocation event including a delayed time for the maximum. This suggests a role in the regulation of the NF-κB nuclear export, which subsequently affects the timing of the second peak (Fig. 3Cii). Finally, the increased class, including our positive
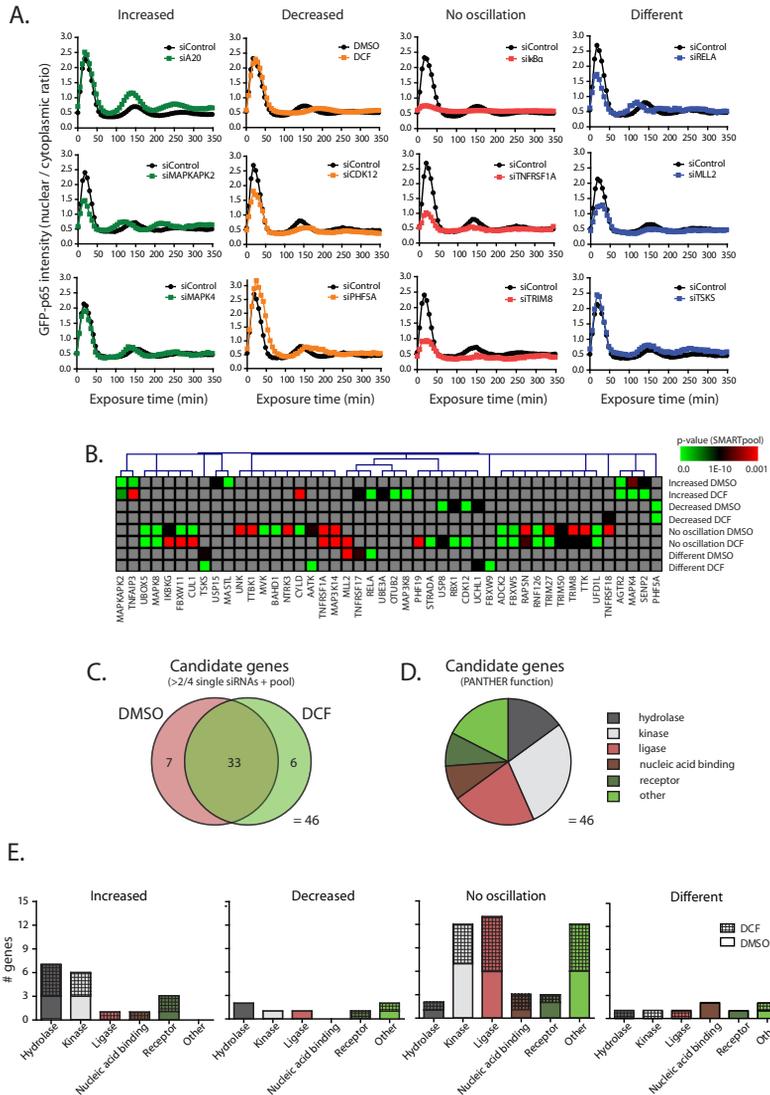
Figure 2. Functional and phenotypic profiling of the siRNA screen hits that control NF-κB oscillation.
(A) Typical non-normalized NF-κB oscillation averages acquired in the deconvolution screen, including examples of knockdowns that led to a phenotype similar to the classification controls; siA20, diclofenac (DCF) and siIκBα. The "different" class is defined by having five or more features significantly different from the siControl. (B) Heatmap of the SMARTpool classification P-values for the hits confirmed by 2 or more single siRNAs in the deconvolution screen, clustered for their corresponding classification on the right. The overlap of the hits under DMSO and DCF conditions are additionally presented in (C). (D) Most of the hits under both DMSO and DCF conditions are described as kinases, (ubiquitin) ligases and hydrolases (mostly deubiquitinases). (E) Knockdown of hydrolases led to a predominantly "increased" phenotype under both DMSO and DCF conditions, while knockdown of kinases and ligases in general lead to "no oscillation" phenotype. The "decreased" phenotype was predominantly detectable under DMSO conditions. The functionality of the target genes was evenly distributed. The "different" phenotype was evenly distributed over functionality as well as exposure condition.

Table 1. Confirmed hits from the deconvolution screen arranged by classification.

Gene Symbol	Name (also known as)	Function	DMSO	DCF	# singles DMSO	# singles DCF	Regulator of NF-κB	Ref
			Decreased					
PHF5A	PHD finger protein 5A	splicing factor	Decreased	Decreased	4/4	3/4	(-)	
UCHL1	ubiquitin carboxyl-terminal esterase L1	hydrolase	Decreased	Different pattern	2/4	4/4	inhibitor	(1)
			Increased					
AGTR2	angiotensin II receptor type 2 (AT2)	receptor	Increased	Increased	3/4	3/4	Activator/inhibitor	(2,3)
MAPK4	mitogen-activated protein kinase 4 (ERK-4)	kinase	Increased	Increased	3/4	2/4	(-)	
MAPKAPK2	mitogen-activated protein kinase-activated protein kinase 2 (MK2)	kinase	Increased	Increased	2/4	2/4	Inhibitor ?	(4)
SENP2	SUMO1/sentrin/SMT3 specific peptidase 2	hydrolase	Increased	Increased	2/4	4/4	Inhibitor/Activator	(5,6)
TNFAIP3	tumor necrosis factor alpha-induced protein 3 (A20)	hydrolase/ligase	Increased	Increased	2/4	3/4	Inhibitor	(7)
RELA	v-rel reticuloendotheliosis viral oncogene homolog A (p65)	nucleic acid binding	Different pattern	Increased	3/4	4/4	Inhibitor	(8)
TNFRSF17	tumor necrosis factor receptor superfamily, member 17 (BCMA)	receptor	Different pattern	Increased	3/4	3/4	Activator	(9,10)
			Stopped					
CDK12	cyclin-dependent kinase 12 (CRK7; CrkRS)	kinase	Decreased	No oscillation	3/4	3/4	(-)	
RBX1	ring-box 1	ligase	Decreased	No oscillation	2/4	2/4	Inhibitor	(11,12)
USP8	ubiquitin specific peptidase 8	hydrolase	Decreased	No oscillation	2/4	3/4	(-)	
TNFRSF18	tumor necrosis factor receptor superfamily member 18 (GITR)	receptor	No oscillation	Decreased	4/4	3/4	Activator	(13)
ADCK2	aarF domain containing kinase 2	unclear	No oscillation	No oscillation	4/4	2/4	(-)	
CUL1	cullin 1	liagse	No oscillation	No oscillation	3/4	3/4	Activator	(14)

Gene Symbol	Name (also known as)	Function	DMSO	DCF	# singles DMSO	# singles DCF	Regulator of NF-κB	Ref
FBXW11	F-box and WD repeat domain containing 11 (BTRCP2)	ligase	No oscillation	No oscillation	4/4	4/4	Activator	(15)
FBXW5	F-box and WD repeat domain containing 5	ligase	No oscillation	No oscillation	3/4	2/4	Inhibitor	(16)
IKBKG	inhibitor of kappa light polypeptide gene enhancer in B-cells kinase gamma (NEMO)	enzyme regulator	No oscillation	No oscillation	4/4	4/4	Activator	(17)
MAP3K14	mitogen-activated protein kinase kinase kinase 14 (NIK)	kinase	No oscillation	No oscillation	2/4	2/4	Activator	(18)
MAPK8	mitogen-activated protein kinase 8 (JNK1)	kinase	No oscillation	No oscillation	4/4	3/4	Inhibitor	(19)
RAPSN	receptor-associated protein of the synapse (rapsyn)	receptor adaptor protein	No oscillation	No oscillation	3/4	3/4	(-)	
RNF126	ring finger protein 126	unclear	No oscillation	No oscillation	3/4	3/4	(-)	
TNFRSF1A	tumor necrosis factor receptor superfamily member 1A (TNFR1)	receptor	No oscillation	No oscillation	4/4	4/4	Activator	(8)
TRIM27	tripartite motif containing 27 (RFP)	ligase	No oscillation	No oscillation	3/4	2/4	Inhibitor	(20)
TRIM50	tripartite motif containing 50	ligase	No oscillation	No oscillation	3/4	2/4	(-)	
TRIM8	tripartite motif containing 8	ligase	No oscillation	No oscillation	2/4	2/4	Activator	(21,22,23)
TTK	TTK protein kinase (PYT)	kinase	No oscillation	No oscillation	3/4	3/4	(-)	
UBOX5	U-box domain containing 5	enzyme modulator	No oscillation	No oscillation	3/4	3/4	(-)	
UFD1L	ubiquitin fusion degradation 1 like	enzyme modulator	No oscillation	No oscillation	4/4	3/4	(-)	
Miscellaneous								
TSKS	testis-specific serine kinase substrate	unclear	Different pattern	Different pattern	3/4	2/4	(-)	

191

Gene Symbol	Name (also known as)	Function	DMSO	DCF	# singles DMSO	# singles DCF	Regulator of NF-κB	Ref
MIL2	myeloid/lymphoid or mixed-lineage leukemia 2	nucleic acid binding	Different pattern	No oscillation	3/4	2/4	(-)	
AATK	apoptosis-associated tyrosine kinase (AATYK)	kinase	No oscillation	Different pattern	4/4	3/4	(-)	
CYLD	cylindromatosis	hydrolase	No oscillation	Increased	4/4	2/4	Inhibitor	(24)
NTRK3	neurotrophic tyrosine kinase receptor type 3 (TRKC)	kinase	No oscillation	Not different	3/4	(-)	(-)	
BAHD1	bromo adjacent homology domain containing 1	nucleic acid binding	No oscillation	Not different	3/4	(-)	(-)	
MVK	mevalonate kinase	kinase	No oscillation	Not different	3/4	(-)	(-)	
TTBK1	tau tubulin kinase 1	kinase	No oscillation	Not different	3/4	(-)	(-)	
UNK	unkempt homolog (unkempt)	ligase	No oscillation	Not different	3/4	(-)	(-)	
FBXW9	F-box and WD repeat domain containing 9	ligase	Not different	Different pattern	(-)	3/4	(-)	
MAP3K8	mitogen-activated protein kinase kinase 8 (COT; TPL2)	kinase	Not different	Increased	(-)	2/4	Activator	(25)
OTUB2	OTU domain ubiquitin aldehyde binding 2	hydrolase	Not different	Increased	(-)	2/4	Inhibitor	(26,27)
UBE3A	ubiquitin protein ligase E3A	ligase	Not different	Increased	(-)	2/4	(-)	
PHF19	PHD finger protein 19	nucleic acid binding	Not different	No oscillation	(-)	3/4	(-)	
STRADA	STE20-related kinase adaptor alpha (STRADalpha)	kinase	Not different	No oscillation	(-)	2/4	(-)	
MASTL	microtubule associated serine/threonine kinase-like (greatwall)	kinase	Increased	Not different	2/4	(-)	(-)	(28)
USP15	ubiquitin specific peptidase 15	hydrolase	Increased	Not different	3/4	(-)	Inhibitor	

DCF: diclofenac.

control TNFAIP3 (A20), the inhibitor of NF-κB activation MAPKAPK2 (25), AGTR2 and MAPK4, were hallmarked by an increase in the number of oscillations, with a decreased time interval between peaks, that exhibit an elevated NF-κB nuclear translocation amplitude (Fig. 3Ciii).
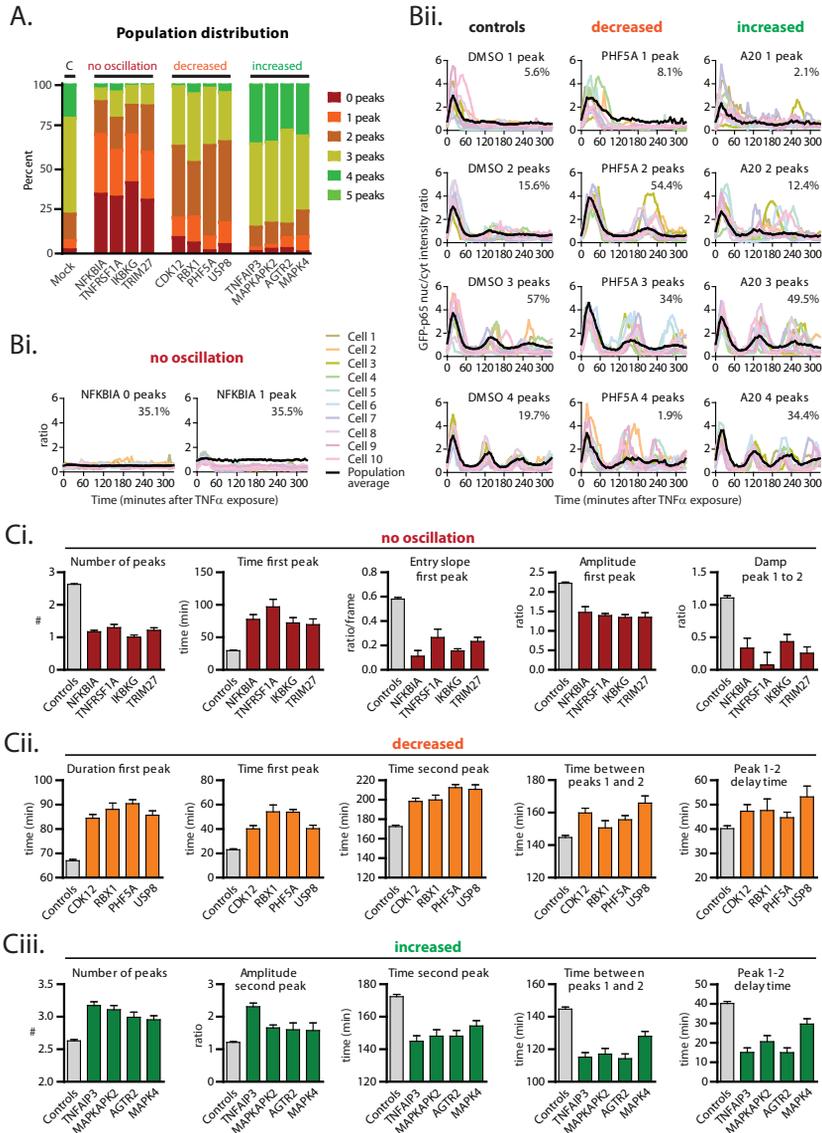

Figure 3. Population statistics. (A) The population distribution of NF-κB oscillations in HepG2 GFPp65 cells upon indicated siRNA treatments. (B) Examples of how each phenotypic class is distributed in relation to the number of translocation peaks. (C) The translocation features that define the different classes: "no oscillation" (Ci), "decreased" (Cii) and "increased"(Ciii) are exemplified by their representative siRNAs.

3.3. Genes that prevent the NF-κB oscillation protect against TNF-α/hepatotoxicant-induced cell death.

Diclofenac (DCF) and carbamazepine (CBZ) are two drugs that are associated with idiosyncratic liver injury in humans, in which the innate immune system-based TNF-α is an important component. Indeed, we have previously reported that diclofenac sensitizes liver cells to apoptosis caused by an otherwise non-toxic dose of TNF-α (5). Since this was directly linked to inhibition of NF-κB signalling (5), we questioned whether inhibition of the 22 candidate genes that showed a "no oscillation" phenotype after knockdown, would affect the cytotoxic response upon DCF/TNF-α and CBZ/TNF-α exposure. Since knockdown of caspase-8 completely inhibited the apoptotic response induced by both DCF/TNF-α and CBZ/TNF-α, we further used this as a positive control (Fig. 4A and B). The majority of the knockdowns that displayed a "no oscillation" phenotype significantly inhibited the drug/TNF-α-induced apoptotic response (12 out of 21; including CDK12, RNF126 and TNFRSF1A), while others did not significantly affect the response (7 out of 21; including CUL1, USP8 and AATK); only IKBKG (IKKγ) and TNFRSF18 knockdowns slightly, but significantly, increased the sensitivity towards apoptosis (Fig. 4B). Interestingly, knockdown of the important negative regulator of TNF-α-induced apoptosis, A20, strongly enhanced the apoptotic response (Fig. 4A and B).

3.4. Protection against apoptosis is correlated to A20 expression and not IκBα activation

A prerequisite for NF-κB nuclear translocation is TNF-α-mediated phosphorylation of IκBα and subsequently targeting of the protein for proteasomal degradation. This IκBα degradation constitutes the earliest negative feedback mechanism for the attenuation of NF-κB activation. We wondered whether genes showing the most significant reduction in drug/TNF-α-induced apoptosis (p-value < 0.001 in Fig. 4B: including CDK12, RNF126, TNFRSF1A, TRIM8 and UFD1L) would affect IκBα levels. Therefore, we used BAC-NFKBIA-GFP (IκBα-GFP) HepG2 cells in which IκBα-GFP is, upon TNF-α treatment, phosphorylated and degraded with the same kinetics as non-tagged IκBα (Supporting Data S2). We individually knocked down the above mentioned genes and followed the IκBα-GFP levels by live cell imaging. Importantly, TNF-α treatment caused an oscillatory response of IκBα-GFP at the population level, corresponding to the western blot data. Depletion of the TNFRSF1A, UFD1L, and RNF126 strongly increased the initial
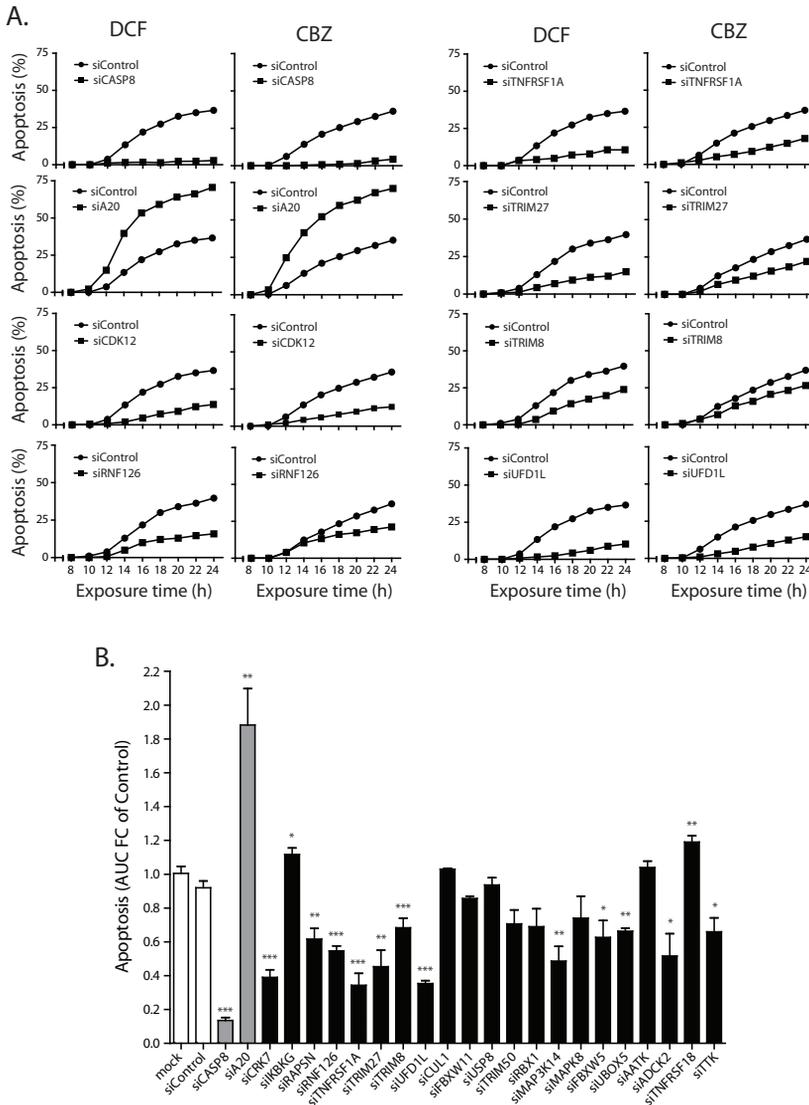
Figure 4. A "no oscillation" phenotype correlates to decreased drug/TNF-α-induced apoptosis. (A) Live apoptosis imaging of wild type HepG2 cells with knockdowns resulting in a "no oscillation" phenotype in GFP-p65 cells after 500 μM diclofenac (DCF) or 500 μM carbamazepine (CBZ) pre-incubation for 8 hours followed by addition of TNF-α (10 ng/ml) The amount of apoptosis is presented as a percentage after normalization to the number of Hoechst33342-positive cells. (B) The area under the curves (AUC) depicted in A was calculated and an average of the fold change (FC) compared to siControl for three independent experiments was determined. The difference in FC AUC compared to siControl was defined using Student's t-test where * P≤0.05, ** P≤0.01 and ***P≤0.001.

levels of IκBα-GFP compared to mock treatment (Fig. 5A), which was associated with an essential complete inhibition of the NF-κB translocation response (see Fig. 2B). As

expected, depletion of the TNF receptor inhibited an IκBα-GFP oscillatory expression. Yet, CDK12, TRIM8 and RNF126 did not affect the initial breakdown of IκBα-GFP, but slightly delayed the newly translated IκBα-GFP. Yet, depletion of CDK12, TRIM8 and RNF126 did not inhibit the early phosphorylation of IκBα upon TNF-α stimulation. As expected, TNFRSF1A knockdown prevented IκBα phosphorylation (Fig. 5B). In contrast, knockdown of UFD1L showed a different response: despite the fact that TNF-α could initiate IκBα phosphorylation, the degradation of IκBα-GFP was reduced, suggesting a role for UFD1L in the degradation of this protein (Fig. 5A and B).

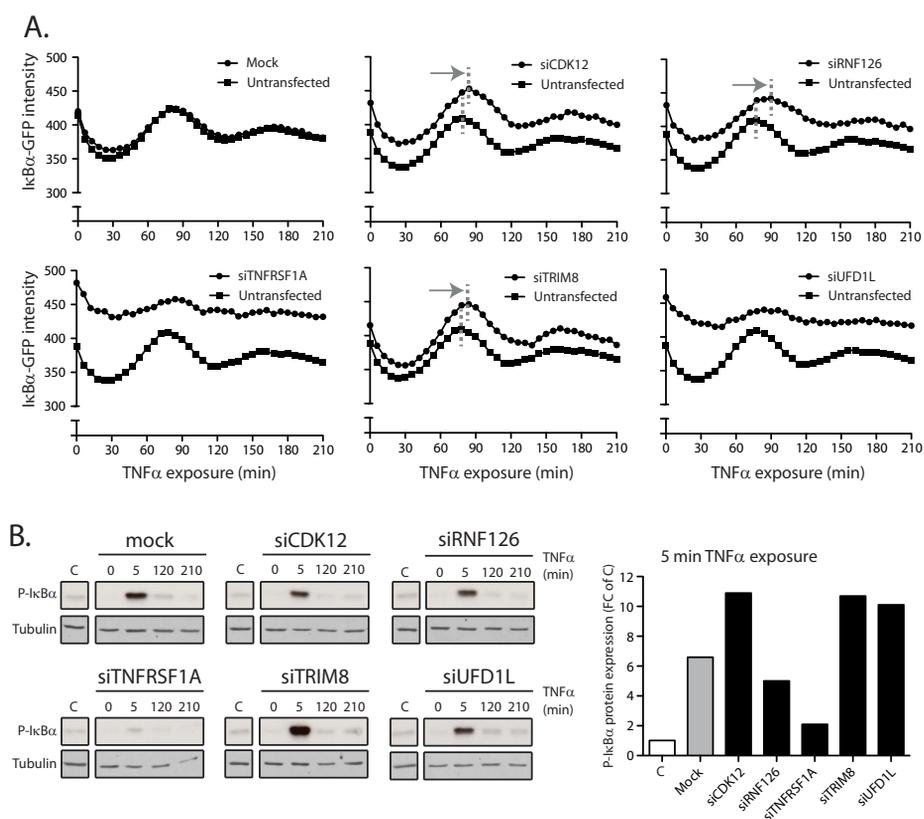**Figure 5. IκBα levels are elevated and the re-expression is delayed while phosphorylation status remains the same after knockdown of the candidate genes.** (A) Quantification of GFP expression in HepG2 cells expressing a BAC-NFKBIA-GFP construct. TNF-α stimulation induces degradation and re-synthesis of the IκBα-GFP protein, which is altered after knockdown of the indicated candidate genes. (B) The amount of IκBα phosphorylation (P) after knockdown of the indicated candidate genes in HepG2 GFP-p65 cells followed by TNF-α exposure for 0, 5, 120 and 210 minutes was determined by western blotting. The tubulin-normalized intensities of P-IκBα for the same knockdowns after 5 minutes of TNF-α exposure is shown in the right panel.

As differences in IκBα phosphorylation and breakdown were not the major contributors to the effect of CDK12, RNF126, TRIM8 and UFD1L, we turned our attention to a second important negative feedback mechanism for NF-κB activity, A20 (TNFAIP3) (17,18). Intriguingly, the A20 levels after knockdown of CDK12, RNF126, TRIM8 or UFD1L were increased at control situation, prior to TNF-α treatment (Fig. 6A and B). Regardless, TNF-α was still capable to further induce A20 after TNF-α exposure (Fig. 6A) most likely since the first NF-κB nuclear entry peak was not affected by these knockdowns. Again, as expected, depletion of the TNF-α-receptor (TNFRSF1A) did not affect A20 levels under control or TNF-α treatment.

A20 was an important regulator of the oscillatory NF-κB response in HepG2 cells. The above data suggested that the effects of CDK12, RNF126, TRIM8 and UFD1L depletion on the reduced NF-κB oscillation was a direct result of the increased A20 levels. To verify this, we performed double knockdown experiments by combining A20 siRNAs with siRNAs against CDK12, RNF126, TRIM8 or UFD1L. A siRNA directed against TNFRSF1A was used as positive control. Importantly, depletion of TNFRSF1A together with A20 did not induce any oscillatory response, indicative for the effectiveness of our double knockdown. Yet, simultaneous knockdown of A20 with either CDK12, RNF126, UFD1L or TRIM8, (partially) recovered the NF-κB oscillatory response (Fig. 7A), which was further quantified with respect to the average number of nuclear entry peaks at the cell population level (Fig. 7B).
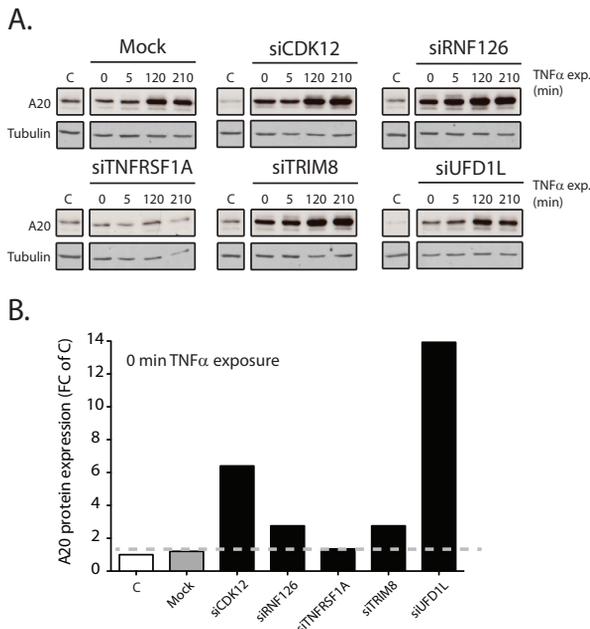

Figure 6. Knockdown of the candidate genes leads to basic upregulation of (de)ubiquitinase A20. (A) Western blot for the A20 expression levels after knockdown of the indicated candidate genes in HepG2 GFP-p65 cells exposed to 10ng/ml TNF-α for 0, 5, 120 and 210 minutes. (B) Quantification of the A20 protein levels at time-point 0 in A.
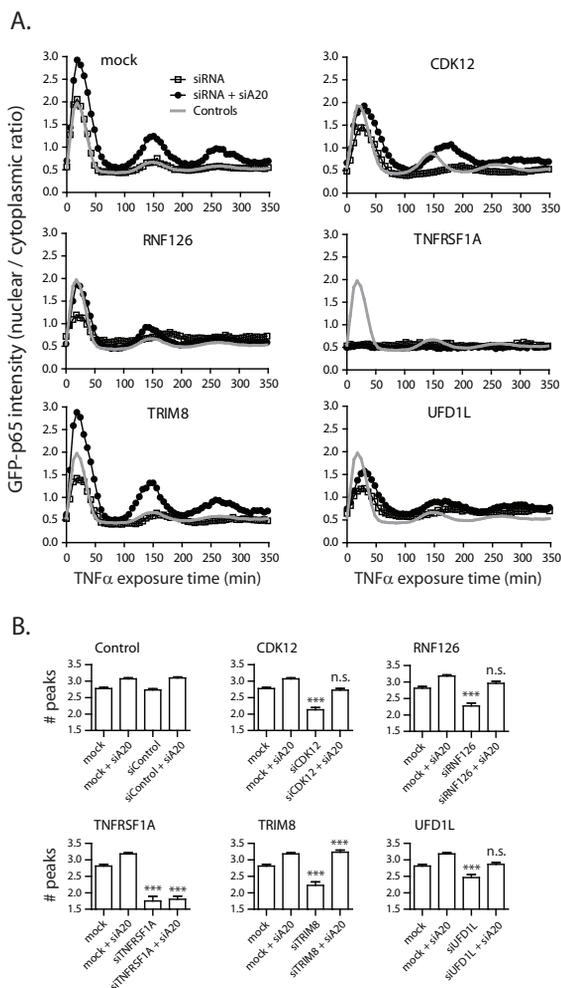
A.

B.

4. Discussion

The transcription factor NF-κB is an important player in both physiology and disease, and its (enhanced) activity has been implicated in cancer as well as chronic inflammatory diseases (2). In addition, inhibition of NF-κB signalling has been implicated in the toxicity of drugs (5). The NF-κB translocation response is tightly controlled by different types of posttranslational modifications such as phosphorylation and especially (de) ubiquitination, which has received much attention in recent years (16, 17). In the current manuscript we have investigated the role of individual kinases, (de)ubiquitinases and sumoylases in the nuclear translocation of the transcription factor NF-κB following

TNF-α stimulation using siRNA-mediated knockdowns. To quantitatively determine the dynamics of the NF-κB nuclear translocation response, we employed a high content imaging method including a recently developed image analysis technique to quantify 32 different parameters describing the NF-κB oscillatory response. Using at least 5 of these features we could distinguish and classify siRNA knockdowns that resulted in a "no oscillation", "decreased", "increased" and significantly "different" NF-κB oscillation phenotype. A siRNA deconvolution screen confirmed 46 of the 115 hits from the primary screen of which the majority showed a "no oscillation" phenotype, and are thus likely to be positive regulators of NF-κB oscillation (Fig. 2). Many of these positive regulators also control the apoptotic outcome after hepatotoxicant/TNF-α-exposure, by regulating the expression levels of the (de)ubiquitinase A20.

We successfully applied an advanced high content imaging approach to identify novel regulators of NF-κB signalling. So far, RNA interference screens for NF-κB signalling mainly involved endpoint assays that mimic NF-κB transcriptional activity using luciferase reporter assays (11, 12), precluding mechanistic insight in the dynamics of the NF-κB activation response. Our method allowed us to identify candidate genes that regulate the oscillatory response of NF-κB. Some of the 46 candidate genes have already been implicated in the regulation of NF-κB signalling (Table 1). This overlap was primarily observed in the target genes that upon knockdown increased or inhibited an NF-κB oscillatory response: genes with an "increased" phenotype were previously described as inhibitors of the NF-κB signalling response, and genes with "no oscillation" phenotypes are associated with promoters of NF-κB signalling (Table 1).

There is increasing evidence for a role of the oscillatory response of NF-κB in the control of gene expression. The total duration of nuclear localization and promoter association is likely to define the spatiotemporal control of epigenetic modulation of genes, and thereby their expression. Indeed, the differential expression of early, mid and late NF-κB target genes seems proportional to the strength and duration of the NF-κB nuclear occupancy (14, 15). IκBα and A20 are classical early NF-κB target genes that are also regulated tightly in our model systems and provide early feedback control of NF-κB activation. At this point we do not know whether our candidate genes that affect the oscillatory response of NF-κB will also affect the overall target gene expression. We anticipate that such a dynamic transcriptional activity of NF-κB is likely to differ within the cell population. Indeed, we observed a differential response of the NF-κB oscillation in our cell population, with around 80% of the cells demonstrating 3 to 4 oscillations in control situations, and only 10% demonstrating one single peak. Depletion of for example TRIM27 completely shifted this response with 80% showing

either 0 or 1 oscillation peak. Reversely, MAPKAPK2, AGTR2 and MAPK4 increased the percentage of cells with 4 peaks. These effects will likely determine NF-κB mediated gene transcription.

Various novel candidates that regulate NF-κB signalling were identified. We described the splicing factor PHF5A as a promoter of the NF-κB oscillatory response. PHF5A is implicated in processing of pre-mRNA (26). We suggest that this gene is required for proper processing of the mRNA of the protein needed for nuclear export of NF-κB, i.e. IκBα, after transcriptional activation. Furthermore we implicated the atypical mitogen activated protein kinase (MAPK) 4 (also known as ERK4), in the attenuation of the NF-κB signalling, since knockdown of this protein resulted in an "increased" translocation phenotype. ERK4 acts as a kinase for the substrate MAPKAPK5 (MK5) (27). We identified MAPKAPK2 (MK2), another protein in the same family as MK5 as an inhibitor of NF-κB translocation. MK2 is known to inhibit the nuclear export of NF-κB by reducing the levels of IκBα (25). MK5 has a similar role as MK2 and both phosphorylate HSP27 (28). Interestingly, HSP27 was previously implicated in the regulation of IKK activity as well as IκBα function (25, 29, 30). More research is required to investigate this link.

Previously we reported that inhibition of the NF-κB translocation is linked to enhanced cytotoxicity following exposure to the hepatotoxicant diclofenac in combination with TNF-α (5). Therefore, we focused on the knockdowns that resulted in a "no oscillation" phenotype. As expected, knockdown of known activators of the NF-κB signalling response, such as IKBKG (IKKγ; NEMO) and TNFRSF18 (GITR) (Table 1) enhanced the apoptotic response under diclofenac/TNF-α and carbamazepine/TNF-α exposure conditions (Fig. 4). In addition, knockdown of known inhibitors of the NF-κB response such as FBXW5 and TRIM27 (RFP) as well as the TNF receptor itself (TNFRSF1A) (Table 1) reduced the apoptotic response (Fig. 4). However, surprisingly, most of the knockdowns that lead to a reduced or no oscillatory response, reduced the drug/TNF-α-induced apoptosis, including the known activators of NF-κB signalling, MAP3K14 (NIK) and TRIM8. Here we report for the first time that this observation is most likely due to the basal induction of the (de)ubiquitinase A20. Higher A20 levels at the start of TNF-α exposure would indeed reduce the induction of NF-κB translocation, as A20 is the most important negative regulator of RIP1 activity (17, 18). Furthermore, since A20 also controls apoptosis by deubiquitinating caspase-8 to reduce the activation of this protease (31), the elevated A20 levels might provide cellular protection against drug/TNF-α-induced cell death. To our knowledge none of the candidate genes have been previously reported to affect A20 expression.

Since both IκBα as well as A20 levels were enhanced under control conditions

(Fig. 5A and 6), and both are important target genes of NF-κB, it seems likely that the enhanced expression of these proteins results from some initial activity of p65 after knockdown of the candidate genes. Especially in UFD1L knockdowns, the A20 and IκBα levels were exceptionally high. UFD1L is described as part of a complex regulating the proteasomal degradation of polyubiquitinated proteins from the endoplasmic reticulum and implicated in the closure of the nuclear envelope (32). Potentially, lack of UFD1L dismantles the boundary between inactive (cytoplasmic) and active (nuclear) p65, allowing a rise in nuclear p65 presence and thereby transcription of the negative feedback genes A20 and IκBα, an effect similar to IκBα knockdown itself (Supporting data S1). In addition, the higher expression of A20 together with potential up-regulation of NF-κB transcribed anti-apoptotic genes could result in the decreased apoptotic response observed.

To our knowledge nothing is known about the functions and substrates of the E3 ubiquitin ligase RNF126. However, as discussed earlier, many regulatory steps leading to the translocation of NF-κB involves ubiquitination of RIP1 and therefore RNF126 knockdown possibly prolongs RIP1 polyubiquitination and thereby NF-κB activity, leading to the "no oscillation" phenotype by up-regulation of A20 as well as IκBα (Fig. 5A and 6). To determine whether the elevated IκBα and A20 expression is indeed caused by enhanced NF-κB activity before TNF-α stimulation, the basal transcriptional activation of NF-κB should be addressed during the pre-stimulation knockdown period.

Similar to PHF5A described earlier, cyclin dependent kinases such as CDK12 have been implicated in the processing of pre-mRNA (33). Although not yet described, knockdown of CDK12 could have a similar effect on the processing of IκBα pre-mRNA as suggested for PHF5A above, resulting in the "delayed" phenotype (Fig. 2A), and delayed re-expression of IκBα protein (Fig. 5A). The delay of IκBα pre-mRNA processing and thus prolonged nuclear p65 presence would also explain the enhanced expression of A20.

TRIM8 is an E3 ubiquitin ligase that has been reported to activate the NF-κB pathway by ubiquitinating the activating kinase TAK1 (34) as well as SOCS-1, a negative regulator of transcriptionally active NF-κB (35, 36). Reduction of TRIM8 thereby resulted in a non-responsive, "no oscillation" phenotype with basic enhanced levels of A20 protein (Fig. 6). Of all candidate gene knockdowns leading to the "no oscillation" phenotype, the effect of TRIM8 knockdown seems to rely most on A20 upregulation as double knockdown for TRIM8 and A20 completely restored and even increased the NF-κB oscillatory response (Fig. 7).

In summary, using an advanced systems microscopy approach involving high

content imaging and RNA interference screening, we identified novel regulators of NF-κB nuclear translocation and possibly signalling. Some of these regulators were essential to control the TNF-α-dependent cell death by controlling the expression levels of the (de)ubiquitinase A20, a negative feedback regulator of TNF receptor signalling. Besides their role in cytotoxicity, our candidate genes are likely to have important functions in inflammation and in the development or progression of different diseases including cancer, rheumatoid arthritis and pathogen infection. This needs further exploration.

Acknowledgements

References

1.   Hayden, M. S., West, A. P., and Ghosh, S. (2006) NF-kappaB and the immune response. Oncogene 25, 6758–6780

2.   Courtois, G., and Gilmore, T. D. (2006) Mutations in the NF-kappaB signalling pathway: implications for human disease. Oncogene 25, 6831–6843

3.   Karin, M., and Lin, A. (2002) NF-kappaB at the crossroads of life and death. Nature immunology 3, 221–227

4.   Shen, H.-M., and Tergaonkar, V. (2009) NFkappaB signalling in carcinogenesis and as a potential molecular target for cancer therapy. Apoptosis 14, 348–363

5.   Fredriksson, L., Herpers, B., Benedetti, G., Matadin, Q., Puigvert, J. C., de Bont, H., Dragovic, S., Vermeulen, N. P. E., Commandeur, J. N. M., Danen, E., de Graauw, M., and van de Water, B. (2011) Diclofenac inhibits tumor necrosis factor-α-induced nuclear factor-κB activation causing synergistic hepatocyte apoptosis. Hepatology 53, 2027–2041

6.   Zhang, L., Jiang, G., Yao, F., He, Y., Liang, G., Zhang, Y., Hu, B., Wu, Y., Li, Y., and Liu, H. (2012) Growth inhibition and apoptosis induced by osthole, a natural coumarin, in hepatocellular carcinoma. PLoS ONE 7, e37865

7.   Israël, A. (2010) The IKK complex, a central regulator of NF-kappaB activation. Cold Spring Harb Perspect Biol 2, a000158

8.   Hayden, M. S., and Ghosh, S. (2008) Shared principles in NF-kappaB signalling. Cell 132, 344–362

9.   Staudt, L. M. (2010) Oncogenic activation of NF-kappaB. Cold Spring Harb Perspect Biol 2, a000109

10.   Halsey, T. A., Yang, L., Walker, J. R., Hogenesch, J. B., and Thomas, R. S. (2007) A functional map of NFkappaB signalling identifies novel modulators and multiple system controls. Genome Biol. 8, R104

11. Chew, J., Biswas, S., Shreeram, S., Humaidi, M., Wong, E. T., Dhillion, M. K., Teo, H., Hazra, A., Fang, C. C., López-Collazo, E., Bulavin, D. V., and Tergaonkar, V. (2009) WIP1 phosphatase is a negative regulator of NF-kappaB signalling. Nature Publishing Group 11, 659–666

12. Li, S., Wang, L., Berman, M. A., Zhang, Y., and Dorf, M. E. (2006) RNAi screen in mouse astrocytes identifies phosphatases that regulate NF-kappaB signalling. Mol. Cell 24, 497–509

13. Ashall, L., Horton, C. A., Nelson, D. E., Paszek, P., Harper, C. V., Sillitoe, K., Ryan, S., Spiller, D. G., Unitt, J. F., Broomhead, D. S., Kell, D. B., Rand, D. A., Sée, V., and White, M. R. H. (2009) Pulsatile stimulation determines timing and specificity of NF-kappaB-dependent transcription. Science 324, 242–246

14. Tian, B., Nowak, D. E., and Brasier, A. R. (2005) A TNF-induced gene expression program under oscillatory NF-kappaB control. BMC Genomics 6, 137

15. Nelson, D. E., Ihekwaba, A. E. C., Elliott, M., Johnson, J. R., Gibney, C. A., Foreman, B. E., Nelson, G., See, V., Horton, C. A., Spiller, D. G., Edwards, S. W., McDowell, H. P., Unitt, J. F., Sullivan, E., Grimley, R., Benson, N., Broomhead, D., Kell, D. B., and White, M. R. H. (2004) Oscillations in NF-kappaB signalling control the dynamics of gene expression. Science 306, 704–708

16. Perkins, N. D. (2006) Post-translational modifications regulating the activity and function of the nuclear factor kappa B pathway. Oncogene 25, 6717–6730

17. Iwai, K. (2012) Diverse ubiquitin signalling in NF-κB activation. Trends Cell Biol. 22, 355–364

18. Wajant, H., and Scheurich, P. (2011) TNFR1-induced activation of the classical NF-κB pathway. FEBS J. 278, 862–876

19. Werner, S. L., Kearns, J. D., Zadorozhnaya, V., Lynch, C., O'Dea, E., Boldin, M. P., Ma, A., Baltimore, D., and Hoffmann, A. (2008) Encoding NF-kappaB temporal control in response to TNF: distinct roles for the negative regulators IkappaBalpha and A20. Genes Dev 22, 2093–2101

20. Puigvert, J. C., de Bont, H., van de Water, B., and Danen, E. H. J. (2010) High-throughput live cell imaging of apoptosis. Curr Protoc Cell Biol Chapter 18, Unit 18.10.1–13

21. Poser, I., Sarov, M., Hutchins, J. R. A., Hériché, J.-K., Toyoda, Y., Pozniakovsky, A., Weigl, D., Nitzsche, A., Hegemann, B., Bird, A. W., Pelletier, L., Kittler, R., Hua, S., Naumann, R., Augsburg, M., Sykora, M. M., Hofemeister, H., Zhang, Y., Nasmyth, K., White, K. P., Dietzel, S., Mechtler, K., Durbin, R., Stewart, A. F., Peters, J.-M., Buchholz, F., and Hyman, A. A. (2008) BAC TransgeneOmics: a high-throughput method for exploration of protein function in mammals. Nat. Methods 5, 409–415

22. Hendriks, G., Atallah, M., Morolli, B., Callêja, F., Ras-Verloop, N., Huijskens, I., Raamsman, M., van de Water, B., and Vrieling, H. (2012) The ToxTracker assay: novel GFP reporter systems that provide mechanistic insight into the genotoxic properties of chemicals. Toxicological Sciences 125, 285–298

23. Takami, Y., Nakagami, H., Morishita, R., Katsuya, T., Cui, T.-X., Ichikawa, T., Saito, Y., Hayashi, H., Kikuchi, Y., Nishikawa, T., Baba, Y., Yasuda, O., Rakugi, H., Ogihara, T., and Kaneda, Y. (2007) Ubiquitin carboxyl-terminal hydrolase L1, a novel deubiquitinating enzyme in the vasculature, attenuates NF-kappaB activation. Arterioscler Thromb Vasc Biol 27, 2184–2190

24. Tan, P., Fuchs, S. Y., Chen, A., Wu, K., Gomez, C., Ronai, Z., and Pan, Z. Q. (1999) Recruitment of a ROC1-CUL1 ubiquitin ligase by Skp1 and HOS to catalyze the ubiquitination of I kappa B alpha. Mol. Cell 3, 527–533

25. Gorska, M. M., Liang, Q., Stafford, S. J., Goplen, N., Dharajiya, N., Guo, L., Sur, S., Gaestel, M., and Alam, R. (2007) MK2 controls the level of negative feedback in the NF-kappaB pathway and is essential for vascular permeability and airway inflammation. J Exp Med 204, 1637–1652

26. Rzymski, T., Grzmil, P., Meinhardt, A., Wolf, S., and Burfeind, P. (2008) PHF5A represents a bridge protein between splicing proteins and ATP-dependent helicases and is differentially expressed during mouse spermatogenesis. Cytogenet. Genome Res. 121, 232–244

27. Kant, S., Schumacher, S., Singh, M. K., Kispert, A., Kotlyarov, A., and Gaestel, M. (2006) Characterization of the atypical MAPK ERK4 and its activation of the MAPK-activated protein kinase

MK5. J. Biol. Chem. 281, 35511–35519

28.   Shiryaev, A., Dumitriu, G., and Moens, U. (2011) Distinct roles of MK2 and MK5 in cAMP/PKA- and stress/p38MAPK-induced heat shock protein 27 phosphorylation. J Mol Signal 6, 4

29.   Parcellier, A., Schmitt, E., Gurbuxani, S., Seigneurin-Berny, D., Pance, A., Chantôme, A., Plenchette, S., Khochbin, S., Solary, E., and Garrido, C. (2003) HSP27 is a ubiquitin-binding protein involved in I-kappaBalpha proteasomal degradation. Mol. Cell. Biol. 23, 5790–5802

30.   Park, K.-J., Gaynor, R. B., and Kwak, Y. T. (2003) Heat shock protein 27 association with the I kappa B kinase complex regulates tumor necrosis factor alpha-induced NF-kappa B activation. J. Biol. Chem. 278, 35272–35278

31.   Jin, Z., Li, Y., Pitti, R., Lawrence, D., Pham, V. C., Lill, J. R., and Ashkenazi, A. (2009) Cullin3-based polyubiquitination and p62-dependent aggregation of caspase-8 mediate extrinsic apoptosis signalling. Cell 137, 721–735

32.   Bays, N. W., and Hampton, R. Y. (2002) Cdc48-Ufd1-Npl4: stuck in the middle with Ub. Curr. Biol. 12, R366–71
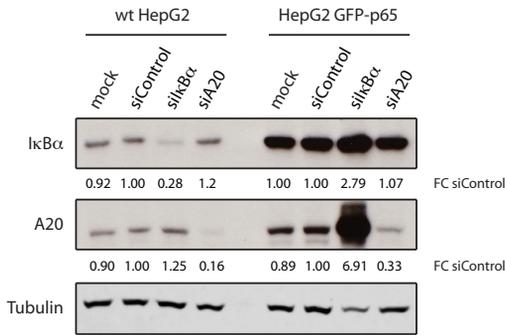
33.   Loyer, P., Trembley, J. H., Katona, R., Kidd, V. J., and Lahti, J. M. (2005) Role of CDK/cyclin complexes in transcription and RNA splicing. Cellular Signalling 17, 1033–1051

34.   Li, Q., Yan, J., Mao, A.-P., Li, C., Ran, Y., Shu, H.-B., and Wang, Y.-Y. (2011) Tripartite motif 8 (TRIM8) modulates TNF-α- and IL-1β-triggered NF-κB activation by targeting TAK1 for K63-linked polyubiquitination. Proc. Natl. Acad. Sci. U.S.A. 108, 19341–19346

35.   Toniato, E., Chen, X. P., Losman, J., Flati, V., Donahue, L., and Rothman, P. (2002) TRIM8/GERP RING finger protein interacts with SOCS-1. J. Biol. Chem. 277, 37315–37322

36.   Strebovsky, J., Walker, P., Lang, R., and Dalpke, A. H. (2011) Suppressor of cytokine signalling 1 (SOCS1) limits NFkappaB signalling by decreasing p65 stability within the cell nucleus. FASEB J. 25, 863–874

Supporting data

	wt HepG2				HepG2 GFP-p65				
	mock	siControl	siIκBα	siA20	mock	siControl	siIκBα	siA20	
IκBα	0.92	1.00	0.28	1.2	1.00	1.00	2.79	1.07	FC siControl
A20	0.90	1.00	1.25	0.16	0.89	1.00	6.91	0.33	FC siControl
Tubulin									

Supporting Data S1. siRNA-mediated knockdown is successful in wildtype and GFP-p65 HepG2 cells. 50 nM siRNA SMARTpool transfection on positive controls, siA20 and siIκBα results in successful knockdown using INTERFERin tranfection reagent, as determined by western blotting. In GFP-p65 cells the siIκBα results in higher IκBα levels after 72 hours of knockdown, since knockdown of this inhibitor leads to enhanced p65 activity during this period and thereby increased IκBα transcription.

Supporting Data S2. Expression of IκBα-GFP does not enhance the levels of the protein. Stable expression of BAC-IκBα-GFP does not result in overexpression of this protein. Furthermore, the GFP-tagged version of this protein behaves as the endogenous protein following TNF-α (10 ng/ml) exposure, as determined by western blotting.

0   0   5   15   30   60   90   120   150   TNFα exposure (min)

- phospho-GFP-IκBα
- phospho-IκBα
- GFP
- IκBα
- Tubulin